Clock Gene Expression in the Eye Exhibits Circadian Oscillation and Light Responsiveness but is Not Necessary for Nocturnal Locomotor Activity of Japanese Loach, Misgurnus anguillicaudatus

Authors: Saratani, Yuya, Takeuchi, Yuki, Okano, Keiko, and Okano, Toshiyuki

Source: Zoological Science, 37(2) : 177-192

Published By: Zoological Society of Japan

URL: https://doi.org/10.2108/zs190110

ZOOLOGICAL SCIENCE **37**: 177–192 (2020)

Clock Gene Expression in the Eye Exhibits Circadian Oscillation and Light Responsiveness but Is Not Necessary for Nocturnal Locomotor Activity of Japanese Loach, *Misgurnus anguillicaudatus*

Yuya Saratani, Yuki Takeuchi, Keiko Okano, and Toshiyuki Okano*

Department of Electrical Engineering and Bioscience, Graduate School of Advanced Science and Engineering, Waseda University, Wakamatsu-cho 2-2, Shinjuku-ku, Tokyo 162-8480, Japan

There are few model fish that are both edible and suitable for use in the laboratory. The Japanese loach (*Misgurnus anguillicaudatus*) is a traditional food in Japan, but is highly neglected despite its great nutritional value. To understand its circadian system and photic input pathway for synchronization of physiological activities to environmental light-dark cycles, we measured locomotor activity under light-dark and constant dark (DD) conditions. Locomotor activity was found to be higher in the nighttime than daytime, and its rhythmicity was weakened under DD conditions. The nocturnal activity of the Japanese loach is mainly controlled by environmental light, rather than the circadian clock. We explored the circadian regulation and light-responsiveness of clock gene expression in the eyes of loaches. The daily expression profiles of its mRNA revealed that most of the examined *Cry* and *Per* genes were likely regulated by internal circadian and/or environmental light signals. Among the *Opsin* genes transcribed in the eye, we detected the retinal photopigment porphyropsin at the protein level, which was lower than in mice. This property of loach eyes prompted us to analyze the locomotor activities of eye-enucleated fish. As a result, they still showed nocturnal circadian activity. Thus, it is likely that extraocular photoreceptive tissue(s) also contribute to the photic input pathway, although loach eyes are a circadian photosensitive tissue. This suggests that the loach mainly uses not its vision but other stimuli, such as mechanical or chemical stimuli, detected by barbels, to coordinate its nocturnal behavior.

Key words: cryptochrome, period, rhodopsin, circadian rhythm, retina

INTRODUCTION

The Japanese loach (*Misgurnus anguillicaudatus*) is widely distributed throughout East Asia, including Japan, and has adapted to the rice paddy environment. Japanese loach is consumed as a traditional Japanese food, and is also used for Chinese folk remedy of hepatitis, osteomyelitis, carbuncles, inflammations, and cancers (Qin et al., 2002). In addition, loach is gaining attention as a feed for the Japanese white stork (*Ciconia boyciana*) and the Japanese crested ibis (*Nipponia nippon*), two rare national species of wild animals in Japan. Thus, the Japanese loach has been recognized as a valuable aquaculture species (Wang et al., 2008). Generally, improvements in the survival rate and growth potential are very important to the development of a successful aquaculture operation (Valente et al., 2013). In terms of growth, it has been reported that the plasma levels of growth factors in the Senegalese sole (*Solea senegalensis*) exhibit a daily rhythm, wherein the physiological effects of exogenous growth hormones are dependent of the timing of their administration (López-Olmeda et al., 2016). These findings highlight the importance of chronobiological aspects in fish aquaculture (López-Olmeda et al., 2016).

The circadian system plays an important role in determining a variety of biological timings, such as the sleep–wake cycle (Huang et al., 2011). Most organisms develop the circadian clock to adapt to environmental light–dark cycles (Panda et al., 2002). In vertebrates, CLOCK:BMAL1 heterodimers bind to E-boxes, and transactivate the E-box-mediated transcription of clock and clock-controlled genes including *Cry* and *Per* (Sato et al., 2006). CRY:PER heterodimer, which closes the core transcription-translation feedback loops to drive an autonomous oscillatory transcription of clock genes over an approximately 24-hour (hr) period (Hastings et al., 2007).

The temporal niche is an important factor for the survival of living organisms. Hence, fish species seem to have changed their active periods along with the changing availability of resources. Such a temporal divergence may be associated with a possible alternation in the interaction between light-input pathway, output mechanisms regulating the locomotor activity, and the central clock oscillator. In mammals, the diurnal/nocturnal modulator in the brain has been well investigated using nocturnal laboratory rats and diurnal *Arvicanthis niloticus* (Schwartz et al., 2004; Mahoney

* Corresponding author. E-mail: okano@waseda.jp
doi:10.2108/zs190110

et al., 2000; Nunez et al., 1999). In fish, the interaction between the clock mechanism and diurnal/nocturnal output is less well understood, probably due to the lack of appropriate nocturnal model species. Zebrafish have been the most extensively used for in vivo and in vitro analyses of clock mechanisms among fish species (Vatine et al., 2011); however, this is a diurnal species (Hurd et al., 1998). As such, in this study, we focused on Japanese loach, which is likely to be nocturnal (Naruse and Oishi, 1994), with small eyes, possibly resulting from an evolutionary adaptation to dark environments. Chronobiological findings on the loach could be applicable to fishery or aquaculture of the loach itself.

In this study, we investigated locomotor activity and the ocular light-input pathway to improve the ecological understanding of the Japanese loach. We measured the locomotor activity of Japanese loaches to confirm that their nocturnality controlled mainly by light. We performed RNA-sequencing and obtained contigs to determine the expression of clock gene mRNA and opsins in loach eyes. Although the expression analysis of clock genes and photopigments strongly suggested the photosensitivity and circadian function of the eye, the photic synchronization of locomotor activity was found to be normal, even after removing the eyes from the fish. Based on these results, the role of the eye for behavior control in the loach was discussed.

MATERIALS AND METHODS

Ethics statement

All experiments were conducted in accordance with the guidelines of Waseda University. All protocols were approved by the Committee for the Management of Biological Experiment at Waseda University, and experimental animal care was conducted with permission from the Committee for Animal Experimentation of the School of Science and Engineering, Waseda University (permission # WD18-052; 2018-A104).

Animals

We used sexually immature loaches unless noted. All loaches were purchased from a local supplier, “Okawa Shoten” (Toyohashi, Aichi 441-8481, Japan; http://dojou-ookawa.com/). The loaches were treated with 50 μg/L malachite green oxalate for one day for disinfection and then kept in breeding tanks under fluorescent light for 12 hr light-dark (LD) cycles (Light:Dark = 12:12, 09:00 Light on, 21:00 Light off). The frozen larva of chironomid “Akamusi” and goldfish pellets were fed at a random time point in the afternoon. The spectrum of the light source (FL25SS EX-D, Panasonic) is shown in Supplementary Figure S1. The temperature of the circulating water was kept between 25.5°C and 26.5°C.

Behavioral experiment

To determine the influence of light on the daily locomotor activity of Japanese loach, their locomotor activity was measured under LD conditions (Light:Dark = 12:12, 09:00 light on, 21:00 light off) for six days and constant dark (DD) conditions for the subsequent 11 days. The measurement apparatus is illustrated schematically in Supplementary Figure S2. In each tank, a white LED (LXK 2-PWC4-0180, Lumileds) was used as a light source (Supplementary Figure S3), and the light intensity at the bottom face was set to between 134.2 μW/cm^2 and 272.0 μW/cm^2.

Rice paddy sand (diameter: about 1 mm; Eiehu Japan Kikaku) was placed on the bottom of the measuring tank for approximately 8 mm (Supplementary Figure S2). Loaches were transferred from the breeding tank to the measuring tank at the end of the light period. Measurement was started at the beginning of the dark period. They were fed at zeitgeber time (ZT) 10 on the third day after the start of the measurement with a water temperature kept between 25.5°C and 26.5°C.

In the eye removal experiment, after seven days measurement under LD conditions, the eyes were removed under ice anesthesia at ZT10–ZT11. After 1-day treatment with 50 μg/L malachite green oxalate, their locomotor activity was measured for seven days under LD cycles.

Tissue collection and RNA preparation for expression analysis of clock genes

Loaches kept at around 25.5–26.5°C and Light:Dark = 12:12 (09:00 light on, 21:00 light off) were divided into an LD group and a DD group. The loaches were transferred from the breeding tank to a sampling tank (approximately 8 L) equipped with a white light (Supplementary Figure S4) at the end of the light period (ZT12) and kept in the dark for 12 hr at 26°C. The loaches in the LD group were then kept in LD for 24 hr, and their eyeballs were removed under ice anesthesia at ZT1 (10:00, n = 6), ZT6 (15:00, n = 5), ZT11 (20:00, n = 6), ZT13 (22:00, n = 5), ZT18 (03:00, n = 4), and ZT23 (08:00, n = 4). The eyes of the loaches in the DD group were also collected at six time points (10:00, n = 4; 15:00, n = 6; 20:00, n = 6; 22:00, n = 6; 03:00, n = 6; 08:00, n = 7) after incubation under DD conditions for 24 hr. Sampling in the light period was performed under fluorescent light (room light, 282.4 μW/cm^2), and sampling in the dark period was performed under dim red light (λ_{peak} = 664 nm, $\lambda_{[5\%]}$ = 625–713 nm, Supplementary Figure S5). Each eyeball was immersed in RNA*later* overnight at 4°C until RNA extraction.

Total RNA was purified according to the recommended protocol of TRIzol® Reagent (Invitrogen). Electrophoresis was carried out to observe the bands of 18S rRNA and 28S rRNA, thereby confirming that the total RNA was not degraded. ReverTra Ace qPCR Master Mix with gDNA Remover (TOYOBO) was used to digest the contaminating genomic DNA in the total RNA and to synthesize cDNA from 500 ng of total RNA, following the manufacturer’s instructions.

Quantitative RT-PCR

Quantitative reverse transcription-polymerase chain reaction (qRT-PCR) was performed using recommended conditions. The relative mRNA levels of the target genes were calculated using the ΔΔCt method, as described previously (Takeuchi et al., 2018). All the PCR products were subjected to 3% agarose gel electrophoresis to verify the appropriate amplification. Primers were designed using Primer 3 (ver. 0.4.0; http://bioinfo.ut.ee/primer3-0.4.0/) (Table 1). Primers were designed in regions with relatively low sequence identities among *Cry* or *Per* genes, and to encompass an intron in the primer or amplification sequence to avoid genomic DNA-derived amplification. The amplification efficiencies of all the primer sets (Table 1) were tested by standard curve analyses using 3-fold serial dilutions ($3^0 - 3^{-6}$) of mixed loach cDNAs. *maEf1α* was used for the reference for its relatively constant expression in the eye.

RNA-sequencing

RNA-sequencing was performed as previously described for the analysis of gold lined spinefoot (Takeuchi et al., 2018) with some modifications: Briefly, brains and eyeballs were excised from three loaches, each at ZT5 and ZT18. The collected tissues were homogenized in TRIzol reagent using an electric homogenizer (Thermo Fisher Scientific). The homogenate was stored at –80°C until further processing. Total RNA was extracted from the homogenate by chloroform extraction, and all the samples were mixed together. Subsequently, genomic DNA was digested with rDNaseI (TaKaRa). Thereafter, total RNA was purified using the miRNeasy Mini kit (Qiagen). The purification method was carried out in accordance with the manufacturer’s instructions.

Library construction and sequencing were performed by

Table 1. Primers used in real-time PCR of *maCry*s and *maPers*.

ID	Length [base]	GC%	5'-sequence-3'	Product size [bp]	Amp. [%]
*maCry1a*_q2F	20	55	CCG CTG TGT GTA CAT CCT TG	230	86
*maCry1a*_q2R	18	55	CCT TCC CAA ATG GCT CAG		
*maCry2a*_F	20	55	GAA TGG ACC CAC CAG AGA TG	181	98
*maCry2a*_R	20	50	GTT AAT GCC TCG GTT TCA CC		
*maCry2b*_q3F	22	50	CTG CGC TGT GTC TAC TTT CTT G	194	98
*maCry2b*_q3R	21	48	CGA TTG ACC TTC CAT TCC TTG		
*maCry3*_q3F2	22	50	GAA GAG CTG GGT TTC AAG ACT C	187	100
*maCry3*_q3R	24	50	CGA ATC GTA GGT AAG GAC TGA GAC		
*maPer1a*_qF	20	50	CTG CCA CCA TGG TCT TTA TG	104	117
*maPer1a*_qR	18	67	ACC TCT CCG CCA CTG TCC		
*maPer1b*_qF	20	55	CAC GGC ACC TTG CAG ATT AC	173	88
*maPer1b*_qR	21	57	CTC GTA GCG TGA GCA GGT AAG		
*maPer2a*_qF	18	56	TAC CGG CGC AGA ATC ATC	230	116
*maPer2a*_qR	22	50	GTT TGT CTG TCG GGA TTC TAG G		
*maPer3*_q2F	21	52	AGA TGG AGA GAT GCG CTA CAG	165	101
*maPer3*_q2R	23	43	GTT GTG CTA AAT ATC CGC TTG TC		
*maEf1α*_F	20	50	TGG TAT GGT TGT GAC CTT CG	175	95
*maEf1α*_R	20	55	GTC GTT CTT GCT GTC TCC AG		

Eurofins Genomics consignment service. A strand-specific library was prepared, and a paired-end sequence was performed using HiSeq 2500 (Illumina). For the adapter, the sequence of TruSeq LT Kits and TruSeq v1/v2 Kits were used. The quality control and filtering of raw reads (89,158,386 reads) were performed using a personal computer (LM-iH610X, mouse computer). Adapter sequences, short reads less than 50 bases, and reads with a lower sequence quality were removed using a PEAT (Li et al., 2015) and Trimmomatic (ver. 0.36) (http://www.usadellab.org/cms/?page=trimmomatic) (Bolger et al., 2014). The clean raw reads were assembled using Trinity (version: 2.8.4) (https://github.com/trinityrnaseq/trinityrnaseq/releases) (Grabherr et al., 2013) Parameters in Trinity were: --seqType fq; --max_memory 200 G; --left read_peat_trim_qf_trim_1.fq; --right read_peat_trim_qf_trim_2.fq; --CPU 24; --min_contig_length 300; --SS_lib_type RF. A BLAST database was constructed from the resultant transcriptome assembly (93,660 contigs).

Molecular phylogenetic analysis of clock proteins

The molecular phylogenetic trees of four clock proteins (CRY, PER, CLOCK, and BMAL) were constructed. First, multiple alignments, including clock protein sequences, were constructed using MEGA (ver. 6.06), removing the N-terminal and C-terminal if necessary. Using the obtained fasta files, molecular phylogenetic trees were constructed by ClustalW (ver. 2.1) and drawn using NJplot (ver. 2.3).

Identification and molecular phylogenetic analysis of opsin proteins

Using 24 zebrafish *Opsin* sequences as queries, tBLASTn analysis was performed against the BLAST database constructed from the Japanese loach transcriptome assembly of brain and eyes (see previous section). We estimated the exon–intron junctions in *maOpsins* from those in zebrafish *Opsin* genes. Based on these results, we designed RT-PCR primers (Table 2), ensuring that at least one exon/intron junction was included in the amplicon.

Expression analysis of *maOpsins*

The total RNA was extracted from eyes of five male and five female loaches per time point (ZT0 (n = 5), ZT6 (n = 5), ZT12 (n = 5), ZT18 (n = 5), and ZT0 (n = 5)), and then ocular cDNA was synthesized as described above. The cDNA pools were mixed together and used as a template for RT-PCR. Genomic PCR was performed by using 10.4 ng of template genomic DNA prepared from the loach muscle. Thermal cycling was initiated with an incubation at 95°C for 30 min; 25 steps of PCR were performed, each one consisting of 95°C for 30 s, 60°C for 30 s, and at 68°C for 2 min. Following the final PCR cycle, the samples were incubated at 68°C for 5 min and kept at 4°C. The PCR products were separated with 3% agarose gel electrophoresis and observed with SYBR Green.

Spectrophotometric analysis

Extraction procedures and spectrophotometric analyses were carried out as described previously (Sakata et al., 2015). All the manipulations were performed under dim red light (> 630 nm). The dissected eyeballs were homogenized with a dounce homogenizer (loose: 30 strokes; tight: 30 strokes) at 4°C in buffer P (50 mM HEPES-NaOH [pH 6.6], 140 mM NaCl, 1 mM DTT, 0.1 mM PMSF, 4 mg/L aprotinin, and 4 mg/L leupeptin). The homogenate was centrifuged at 15,000 rpm for 30 min, and the pellet was collected. To solubilize ocular pigments, the pellet was homogenized again (tight: 30 strokes) in 1% CHAPS/buffer P. After centrifugation at 15,000 rpm for 30 min, the clear supernatant was collected and subjected to spectrophotometry using a SHIMADZU UV-2450 spectrophotometer. The sample was kept in an optical cell (light path, 1 cm) at 4°C during the analysis. After measuring the absolute absorbance, hydroxylamine (NH_2OH-HCl, pH 6.6) was added to the sample at a final concentration of 100 mM. The sample was kept for 120 min until the spectral changes disappeared. Then, the photopigments in the sample were bleached by successive irradiations with red and green light (Supplementary Figures S6 and S7).

Immunoblot analysis

SDS-PAGE and immunoblotting analyses were performed as described previously (Sakata et al., 2015; Watari et al., 2012; Toda et al., 2014). A small aliquot (704 ng) of the loach ocular extract for spectrophotometric analyses (see above) was used. Affinity-purified anti-chicken rhodopsin antiserum (cRh-C antibody (Sakata et al., 2015)) or control mouse IgG (I5381-1MG; Sigma) were used as the primary antibody.

Immunohistochemistry

Sample treatment, processing, and immunohistochemical procedures were performed as described previously (Watari et al., 2012). Loach heads were collected at ZT18 and stored at −80°C until use. The frozen samples were sectioned transversely at 14 μm. After blocking with 1.5% horse normal serum in 0.05% Triton X-100/PBS (PBS; 10 mM Na-Phosphate [pH 7.4], 140 mM NaCl, 1 mM $MgCl_2$) for 1 hr at room temperature, the slides were incubated for 16 hr at 4°C with primary antibody (cRh-C or control mouse IgG). The samples were rinsed with 0.05% Triton X-100/PBS, and then treated with a biotinylated anti-mouse IgG for 1 hr at

Table 2. Primers used in RT-PCR of *maOpsin*s.

ID	Length [base]	GC%	5'-sequence-3'	Product size [bp]
*maGreen-opsina*_F	21	48	GAT TTC CTC GGC TGT TAA TGG	363
*maGreen-opsina*_R	20	50	GGG ACA AAG AAA TGG CAG AC	
*maGreen-opsinb*_F	22	45	GGA GCT TCA AAT TCT CAT CAG G	233
*maGreen-opsinb*_R	20	50	GAA AAA GAT GAC GGC GAC TG	
*maRh1*_F	21	52	CAG TGC TCA TGT GGA GTT GAC	249
*maRh1*_R	21	43	CAG CCA ACA AAT CAA GAA AGC	
*maRh1-2*_F	24	50	TCT TGT GCT ATA CCC CCT CTA GTC	335
*maRh1-2*_R	22	50	GTG AAG ATG TAC CAA GCT ACG C	
*maExorh*_F	25	40	TTA CTA CAC ACC AAA ACC TGA GTT C	281
*maExorh*_R	22	41	CAA ATT CTG CAC CTT GAT TAG C	
*maUV-opsin*_F	22	45	CAT CGT CCT CTT CGT TAC ATT G	312
*maUV-opsin*_R	20	60	GTG AGG GCT ACT GCT CCA AG	
*maRed-opsin*_F	21	52	GTC GTT GCT TCT GTC TTC ACC	324
*maRed-opsin*_R	18	50	AGC AGA TGC CCA TTT TGC	
*maBlue-opsin*_F	25	40	CAC TCA TGC TAT AAT TGG CTG TAT C	209
*maBlue-opsin*_R	20	50	CAA TGG TGC TGA AAG GAA CC	
*maValb*_F	20	55	ACT TCT TTC TGG GCG TCT GG	294
*maValb*_R	23	48	TGT GGT CAT AGT AGT TGG TCG AG	
*maPara*_F	20	55	ACT GGC AAG GTC GAG ACT TC	264
*maPara*_R	20	50	GGA CAT CGG GAT TAA AGA CG	
*maOpn4x1*_F	20	50	TAA TCG GGG CTT TAG GGA TC	151
*maOpn4x1*_R	20	45	ACA AAG AAG ATG GGC GAT TG	
*maPeropsin*_F	18	56	TGG TGC TGC TGA TGT TCG	167
*maPeropsin*_R	20	55	GAT CTG GCA ACC CAT GTA GC	
*maOpn4m1*_F	20	55	CTC TCA TGG TCA TCG CAG TG	107
*maOpn4m1*_R	19	58	CCA GGC TCC CAG AAG AAT C	
*maOpn4m3*_F	18	56	CGT CAT GTC ACG CAA ACG	313
*maOpn4m3*_R	22	45	CTT CTT GAT GGA GTC TTT GTG C	
*maOpn4m2*_F	20	55	ACG CAC TGG TGA TCT ACG TG	118
*maOpn4m2*_R	20	50	AAC ATT GGT GCT TGG GTG AG	
*maOpn4x2*_F	22	45	ACC TCC ATG ATA AAC CTG TTG G	237
*maOpn4x2*_R	20	55	ACT TCT GTT GGC TGG AGA GG	

room temperature. After washing with 0.05% Triton X-100/PBS and PBS, the immunoreaction was enhanced by applying the Avidin-Biotin Complex method using Vectastain Elite ABC kit (vector laboratories) for 30 min. The resulting signals were visualized via treatment with DAB-peroxidase substrate solution (0.05% diaminobenzidine, 0.01% H_2O_2, 50 mM Tris-HCl [pH 7.4], 200 mM NaCl, 1 mM $MgCl_2$) for 3 min at room temperature.

Statistical analysis

The locomotor activity data were analyzed by using Actogram J software (Schmid et al., 2011) to obtain actograms and chi-squared periodograms, from which the period lengths were estimated with probabilities of less than 0.01. Amplitude of the estimated period length in the chi-squared periodgram was used to calculate Q value that indicates robustness of rhythmicity. A Wilcoxon's signed-rank test (significant $P < 0.05$) was used to compare the Q values of the estimated period-lengths in LD with those in DD, or those of intact fish with those of eye-excision fish. Two-way factorial ANOVA was used (significant $P < 0.05$) to test the variations of locomotor activity and gene expression levels. The Tukey-Kramer method was used for multiple comparisons (significant $P < 0.05$).

RESULTS

Locomotor activity analysis of Japanese loach under the LD and DD conditions

We investigated the diel locomotor activity of Japanese loach in the laboratory environment (Fig. 1, Supplementary Figure S8 and Supplementary Table S1). Each fish was reared under LD condition for six days, then kept under DD conditions for 11 days. Chi-squared periodograms showed that 13 out of 14 animals had significant 24-hr rhythmicity with periods of 23.6–24.7 hr under LD condition (Fig. 1A–K, M, and N; LD in middle rows), indicative of the synchronization of their locomotor activities to the LD cycles. Their locomotor activity rhythmicity under the DD condition decreased compared to LD condition, except for Fig. 1J and L (Fig. 1, middle rows and Supplementary Figure S8). In the analyses of their locomotor activities with 4-hr time windows (Fig. 1, bottom rows), a significant interaction between light conditions and circadian time was observed in five of 14 individuals (Fig. 1A, C–E, and H; *s. i.* in bottom rows). In these animals, under LD conditions, the locomotor activity during each time point of the light phase was significantly lower than or not higher than those of the dark phase (Fig. 1A, C–E, and H; grey line in bottom rows).

The locomotor activity of the other nine animals did not show significant interactions (Fig. 1B, F, G, and I–N; bottom rows). Among them, six individuals showed significant daily variation (Fig. 1B, G, J, K, M, and N; daggers in bottom rows), and the locomotor activity during each time point of ZT/CT0-ZT/CT12 was significantly lower or not higher than those of ZT/CT12-ZT/CT24 in five of the six animals (Fig. 1B, G, J, K, and M; dashed line in the bottom rows). The locomotor activity under the LD condition was higher than that under the DD condition in three of the nine animals (Fig. 1F, L, and N; asterisks bottom rows). One individual did not show significant differences in either circadian time or light conditions (Fig. 1I).

Phylogenetic analysis of clock proteins

Japanese loach exhibited nocturnal behavior under the LD condition, however, the rhythmicity was weakened or lost in DD (Fig. 1), implying that locomotor activity is predominantly controlled by light. Commonly, the eye is the primary

site for the input pathway of visual and non-visual light information, such as time signals, while the brain and even peripheral tissues are photosensitive in fish species (Whitmore et al., 2000; Moore and Whitmore, 2014). Therefore, we considered the eyes to be a plausible candidate for the photoreceptive site involved in the suppressive photoresponses, although loach eyes are rather small. Therefore, we verified the photic and circadian function of the loach eyes by determining the expression of both clock genes (Figs. 2 and 3) and the photopigments (Figs. 4–6).

As transcriptome data for the central tissues has yet to be reported, we performed an RNA-sequencing of the central nervous tissues (eyes and brain) prior to the measurement of the expression profiles of clock genes in the loach eye (Long et al., 2013; Luo et al., 2015; Huang et al., 2016). We locally constructed a BLAST database from the transcriptome assembly to identify the transcripts encoding cryptochrome/photolyase and clock (-related) proteins (see

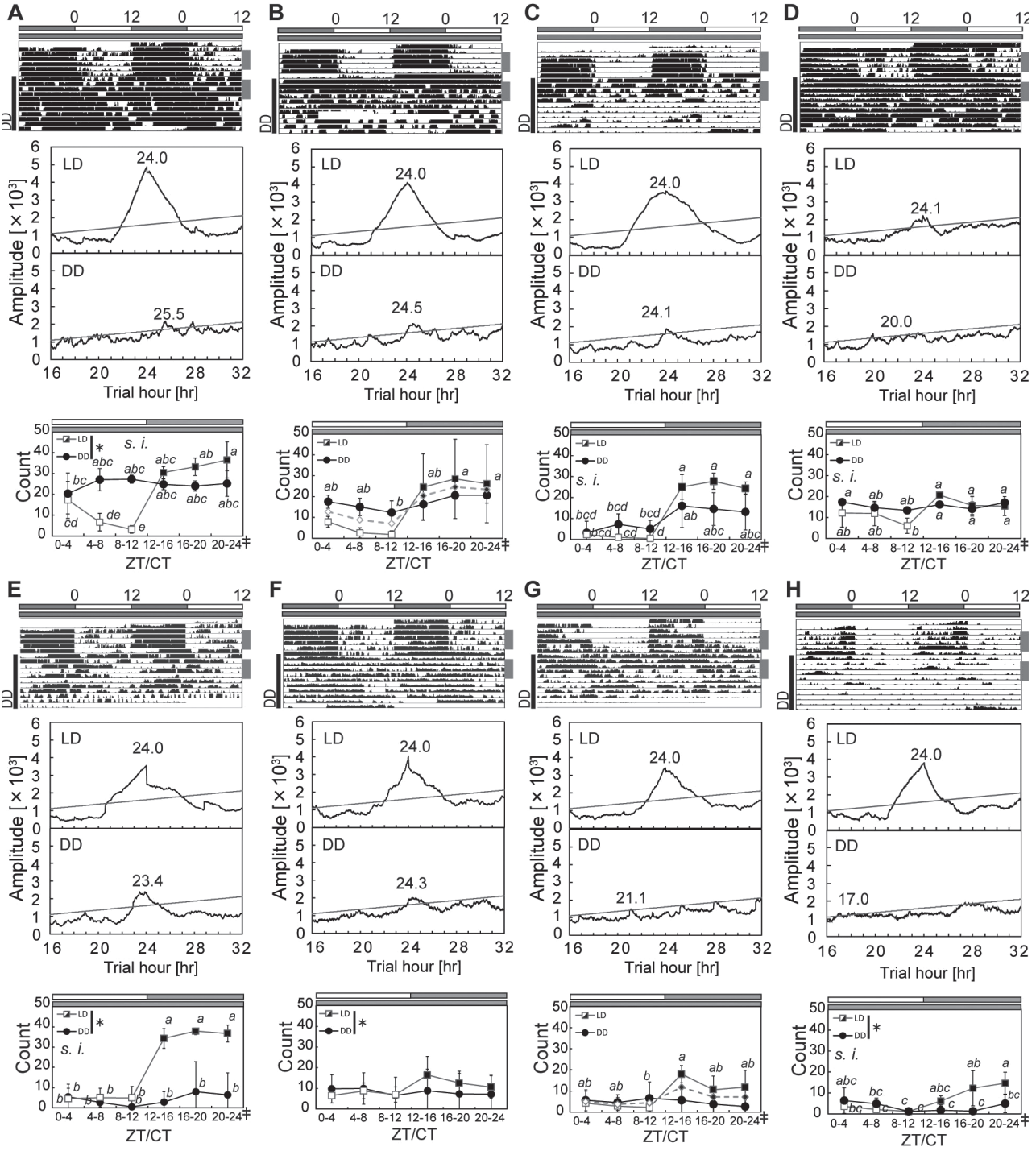

Fig. 1. Continued.

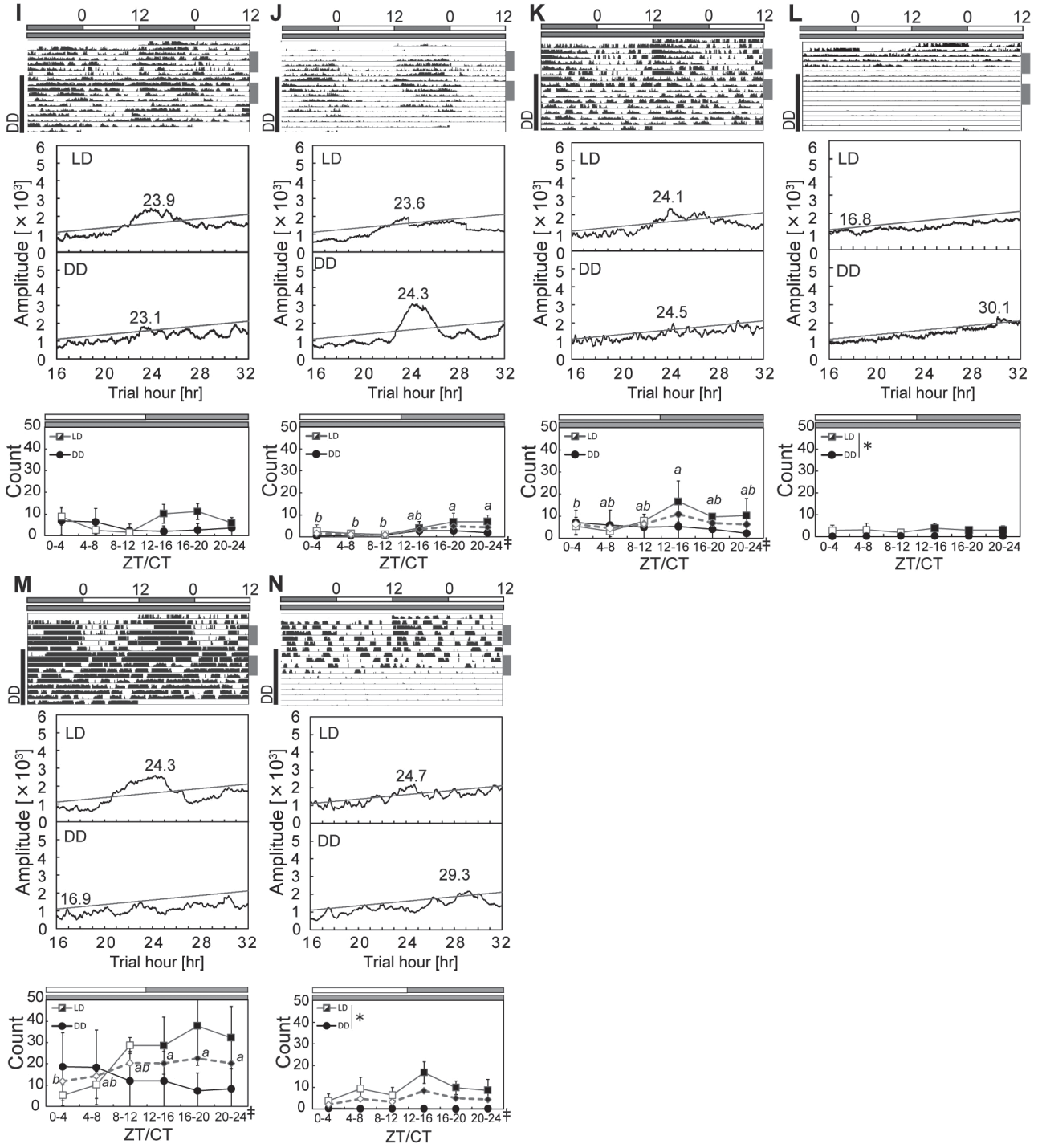

Fig. 1. Locomotor activity of Japanese loach under LD and DD conditions. Top rows: Double-plot actograms of locomotor activity of 14 Japanese loaches under LD and DD conditions. The locomotor activity of each fish was measured for six days in LD (12:12) and subsequently for 11 days in DD (shown by a vertical black bar on the left side). Middle rows: Chi-squared periodograms of the locomotor activities. Significance lines ($P < 0.01$) are colored in grey. The presumed free-running periods under the DD condition are shown. Bottom rows: Analyses of the locomotor activity in a 4-hr window. Circadian time (CT) was estimated by the free-running period. One cycle was divided into six equal periods. Locomotor activity of four daily or circadian cycles (shown by grey bars on the right side of double-plot actograms) were averaged for each period (counts ± SD per min) and plotted by grey lines with squares (LD) or black lines with black circles (DD). The solid and open squares represent dark and light points in LD cycles, respectively. The significance of the interaction between the circadian rhythm and light conditions was examined by two-way factorial ANOVA and was considered a significant interaction (*s.i.*) if the *P*-value was less than 0.05. Multiple comparison tests were performed using the Tukey-Kramer method. Asterisks and daggers represent significant variations depending on the light conditions and time periods, respectively. Different letters indicate significant differences between comparisons ($P < 0.05$). Dashed lines represent the averaged locomotor activities under the LD and DD conditions. They were drawn when a significant interaction was not detected. Significant daily variations were detected using two-way factorial ANOVA.

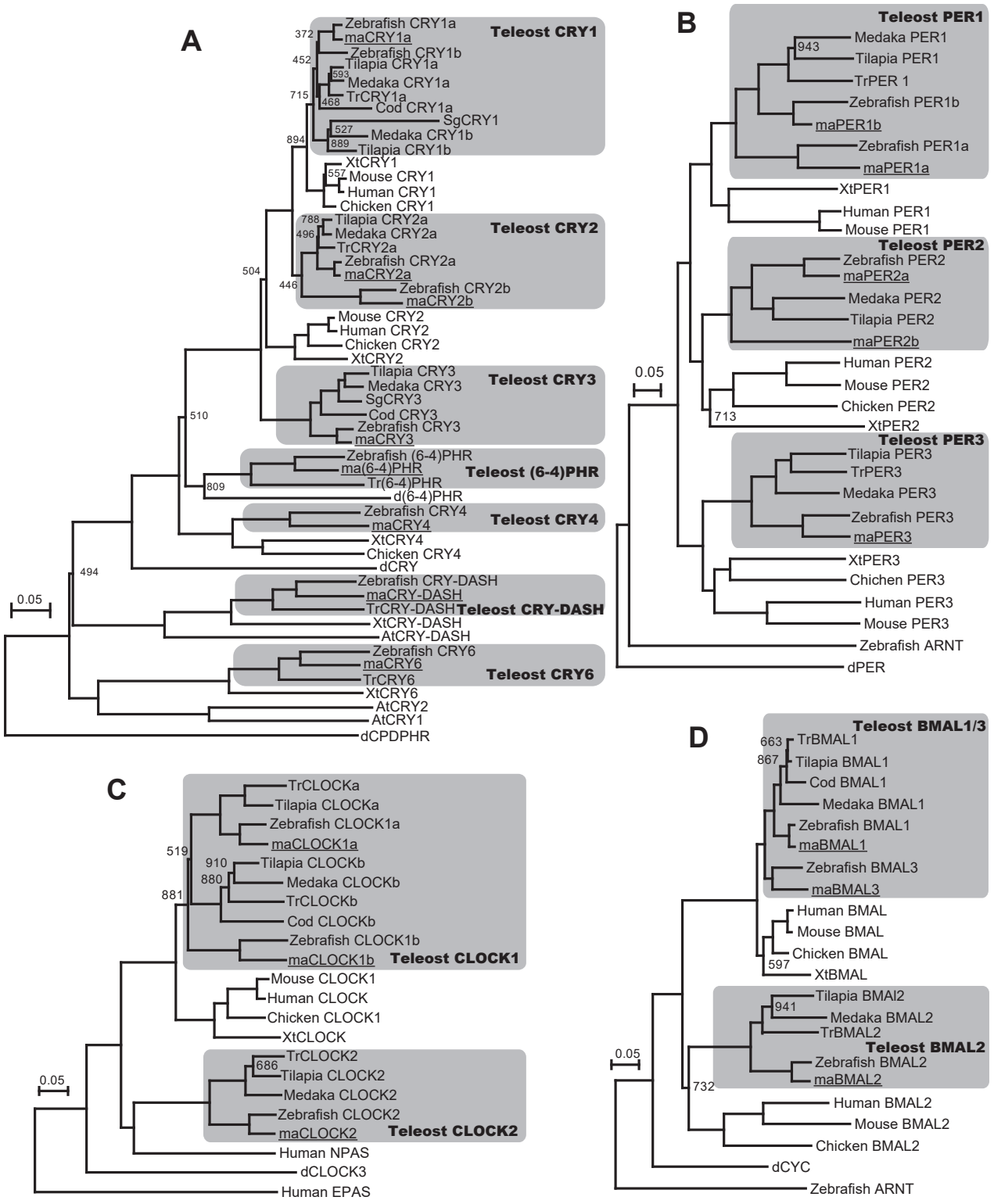

Fig. 2. Molecular phylogenetic trees (NJ trees) of loach clock proteins. **(A)** A molecular phylogenetic tree of CRY proteins. **(B)** A molecular phylogenetic tree of PER proteins. **(C)** A molecular phylogenetic tree of CLOCK proteins. **(D)** A molecular phylogenetic tree of BMAL proteins. Molecular phylogenetic trees were constructed using the Neighbor-Joining method (ClustalW ver. 2.1). The values at the branches indicate bootstrap probabilities. Bootstrap values > 95% have been omitted. Multiple alignments were made using MEGA 6.06. Because some of amino acid sequences obtained from the transcriptome database did not cover the entire CDS, the N-terminus and/or C-terminus of the alignment were manually omitted, and then the processed alignments (corresponding to Val^{2}–Ser^{504} in zCRY1aa [panel A], Met^{1}–Gln^{668} in zPER1a [panel B], Met^{1}–Gln^{892} in zCLOCK1a [panel C], and Met^{1}–Leu^{626} in zBMAL1 [panel D]) were subjected to progressive alignment by using ClustalW ver. 2.1, (DDBJ) to generate molecular phylogenetic trees. Tr, *Tetraodon nigroviridis*; Sg, *Siganus guttatus*; Xt, *Xenopus tropicalis*; ma, *Misgurnus anguillicaudatus*; d, *Drosophila melanogaster*; At, *Arabidopsis thaliana*.

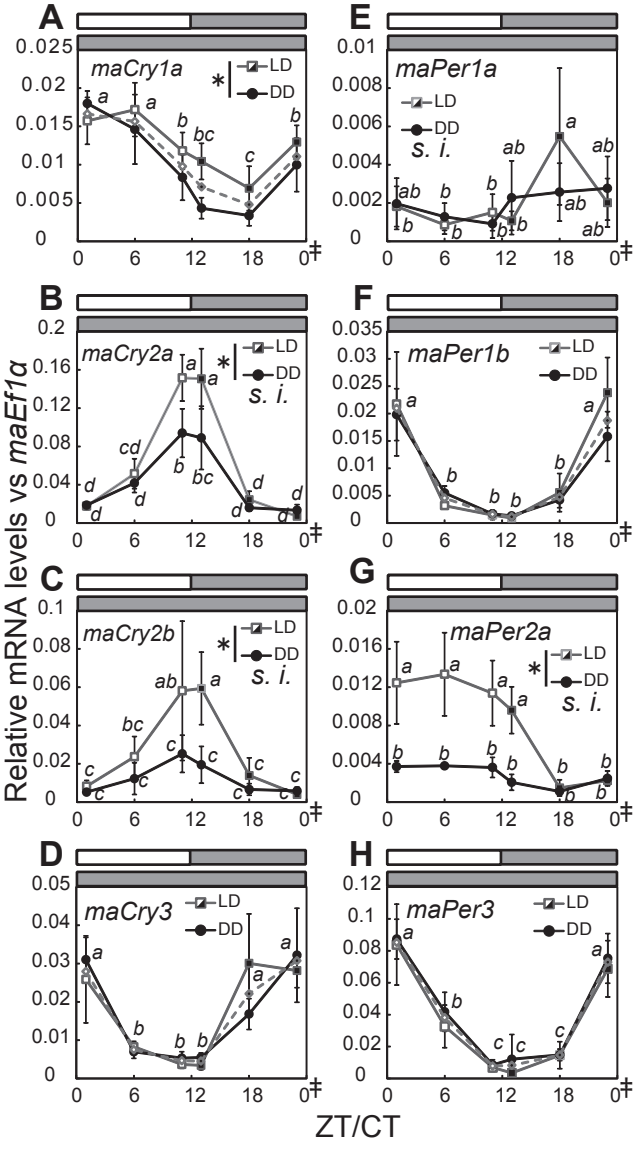

Fig. 3. mRNA expression levels of *maCrys* and *maPers* under the LD and DD conditions. Grey and black lines denote mRNA profiles under the LD and DD conditions, respectively. Solid and open squares represent dark and light points, respectively. The messenger RNA levels of *maCrys* and *maPers* were calculated as a value relative to the *maEf1*α expression levels. Expression levels of each clock gene were compared between all populations using two-way factorial ANOVA followed by Tukey-Kramer multiple comparison test ($P < 0.05$). Different letters indicate significant differences between comparisons. Asterisks indicate significant differences between LD and DD conditions. Daggers indicate significant differences among time points. Dashed lines represent the average of the mRNA expression levels under the LD and DD conditions. They were drawn when significant interactions were not detected. Significant daily variations were detected by two-way factorial ANOVA. Mean values ± SD were plotted.

below). Phylogenetic analyses located the partial sequences close to their orthologous genes of zebrafish in molecular phylogenetic trees (Fig. 2 and Supplementary Table S2). The transcriptome datasets generated and/or analyzed during the current study are available in the DDBJ repository (Accession: DRA007566).

Zebrafish has nine *Cry* genes (*zCry1a*, *zCry1b*, *zCry2a*, *zCry2b*, *zCry3*, *z(6-4)phr*, *zCry4*, *zCry6*, and *zCry-dash*) and four *Per* genes (*zPer1a*, *zPer1b*, *zPer2*, and *zPer3*), which may have diverged over the course of three whole genome duplications, which occurred at an early stage of vertebrate (teleost) evolution (Inoue et al., 2015; Sato and Nishida, 2010). The topologies of the phylogenetic trees (Fig. 2) showed no discrepancy based on their taxonomic relationships. As a result of the tBLASTn search of the database, along with the following comparison with zebrafish *Cry* genes, we identified eight loach paralogs of *zCry* (*Misgurnus anguillicaudatus Cry1a* [*maCry1a*], *maCry2a*, *maCry2b*, *maCry3*, *ma(6-4)phr*, *maCry4*, *maCry6*, and *maCry-dash*) (Fig. 2A). Similarly, we identified five loach paralogs of *zPer* (*maPer1a*, *maPer1b*, *maPer2a*, *maPer2b*, and *maPer3*) (Fig. 2B), three paralogs of *zClock* (*maClock1a*, *maClock1b*, and *maClock2*) (Fig. 2C), and three paralogs of *zBmal* genes (*maBmal1*, *maBmal2*, and *maBmal3*) (Fig. 2D). We did not identify a *zCry1b* ortholog in the loach transcriptome sequences, possibly due to the lack of *Cry1b* or the very low expression levels in the central nervous tissues.

Expression analyses of loach clock genes under LD and DD conditions

To determine whether the expression of clock genes is controlled by environmental light and/or the internal circadian oscillator, we measured the transcript levels in the eye by qRT-PCR (Fig. 3 and Table 1). We measured the mRNA levels of four *Cry* (orthologs of animal *Cry1/2*) and four *Per* genes in the eyes, which were collected at six time points under LD or DD conditions (Fig. 3 and Supplementary Table S3).

In *maCry1a* (Fig. 3A), daily fluctuations were observed, with higher expression levels in LD compared to DD. The expression levels of *maCry2a* (Fig. 3B) showed daily changes, with a peak in the evening (ZT11–ZT13), and the mRNA levels at these points were significantly higher in LD than DD. Significant variations were observed even under the DD condition (Fig. 3B, black circles). These results suggest that the ocular expression of *maCry1a* and *maCry2a* are likely regulated by both the circadian clock and external light signals. *MaCry2b* mRNA levels (Fig. 3C) increased during the light period under LD condition, similar to *maCry2a*, but did not show any significant fluctuations in DD, implying photic regulation.

No significant interactions between daily temporal variations and light conditions were detected in *maCry3*, *maPer1b*, and *maPer3* (Fig. 3D, F and H), all of which in turn showed clear daily changes independent of light conditions, indicative of circadian regulation. *MaPer1a* showed significant interactions between daily temporal variations and light conditions; however, neither photic nor circadian variations were observed (Fig. 3E). The mRNA levels of *maPer2a* were significantly higher in the light and just after dark (ZT1–ZT13 in LD, Fig. 3G) than the other points in the dark (ZT1–ZT23 in DD; ZT18 and ZT23 in LD), indicating light-dependent upregulation.

Identification and molecular phylogenetic analysis of *maOpsins*

We determined the types of *Opsin* genes that were

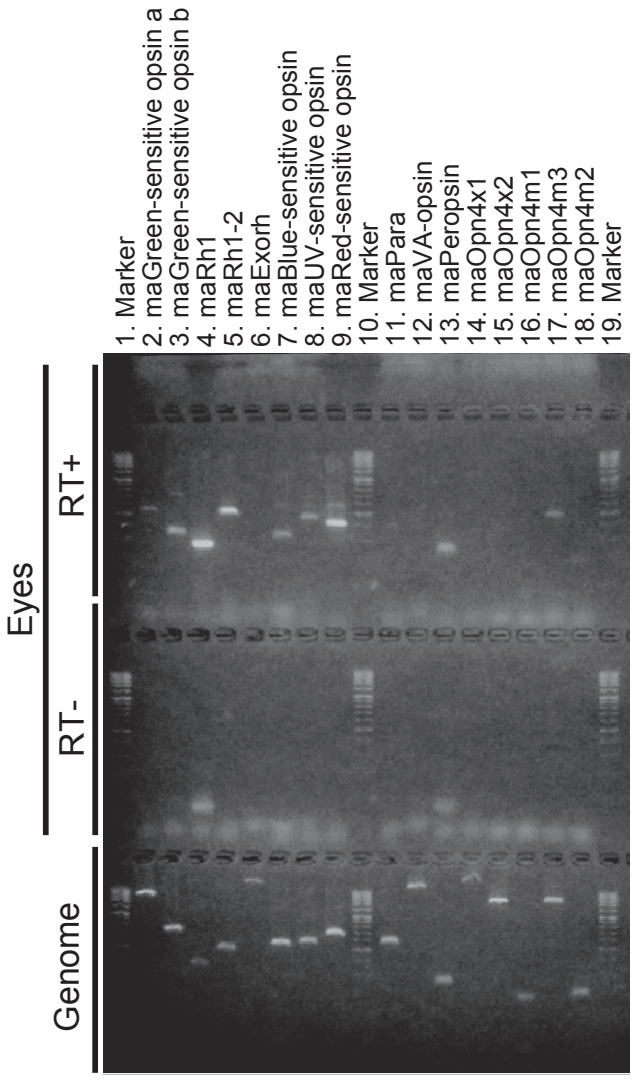

Fig. 4. PCR analysis of loach *Opsin* genes. PCR was performed in the presence of eye cDNA template (top row), genomic DNA template (bottom row), or in the absence of eye cDNA template (middle row). PCR products were separated with 3% agarose gel electrophoresis and observed with SYBR Green.

expressed in the eye by RT-PCR. Firstly, we performed tBLASTn analysis to identify *Opsin* transcripts using our transcriptome assembly, and found 21 contigs which could possibly encode *Opsins* (Supplementary Table S4). We next designed primers for RT-PCR to examine their presence in the loach genome and expression in the eyes (Table 2).

For 16 of 21 primer sets, we detected single amplified products in genomic PCR (Fig. 4, Genome). Then, the contigs corresponding to the 16 primer sets were assumed to exist in the loach genome and divided into several groups by molecular phylogenetic analysis (Fig. 5). We identified seven visual *Opsin* genes (five cone opsins and two rhodopsins) and nine non-visual *Opsin*s. Except for three primer sets (*maPeropsin*, *maOpn4m1*, and *maOpn4m2*; lanes 13, 16, and 18, respectively), the band sizes were larger than those estimated from the transcriptome, probably because all of the primer sets were designed to amplify the genomic DNA encompassing introns. As for the *maPeropsin*, *maOpn4m1*, and *maOpn4m2* genes, these may be single-exon genes, as in zebrafish *Opn4m2* (Davies et al., 2011), or alternatively, the amplified regions contain very short introns.

Next, the expression levels of the 16 *maOpsin* genes in the eyes were investigated by RT-PCR using ocular cDNA as a template (Fig. 4, Eyes, RT+). Single bands were detected for visual *Opsin*s (Fig. 4, lanes 2–5 and 7–9), among which the intensity of the bands for *maRh1*, *maRh1-2*, and *maRed-opsin* (Fig. 4, lanes 4, 5, and 9) were relatively higher than those for the other genes. This indicated the relative abundance of these mRNAs, although the present RT-PCR analysis is not highly quantitative. Among non-visual *Opsin* genes, single bands were detected for *maPeropsin* (lane 13) and *maOpn4m3*, (lane 17) and weak signals were observed for *maParapinopsin* (*maPara*, lane 11) and *maOpn4m2* (lane 18). Although the RT-PCR bands of *maPeropsin* and *maOpn4m2* had almost the same mobility as those obtained using genomic PCR, we considered only the signals originating from cDNA due to the lack of their bands in control experiments, excluding the RT reaction (Eyes, RT-). We did not detect any expression of other non-visual *Opsin* genes, including the pineal-specific rhodopsin *Exorh* (lane 6).

Immunohistochemistry of retina and spectrophotometry of eyeball extract

The detection of opsin protein(s) in loach eyes was performed by western blot, immunohistochemistry, and spectroscopy. MaRod-opsin protein in the loach eyeball extract was analyzed by western blot analysis using an affinity-purified anti-chicken rhodopsin antiserum (cRh-C antibody (Sakata et al., 2015)). A rhodopsin-like immunoreactive band was observed at a mobility of 39 kDa (Fig. 6A), which is likely to correspond to the monomer of rhodopsin or porphyropsin, a photopigment found in the retinal rods of freshwater fish, using A_2-retinal (dehydroretinal) as the chromophore instead of A_1-retinal. Additional bands were found at a mobility of 86 kDa, as well as the higher positions in both the loach eyeball extract and purified chicken rhodopsin, which were considered to be dimers and multimers of those opsins. In the immunohistochemistry analysis, rhodopsin-like immunoreactivities were found in many rods in the retina (Fig. 6B–E).

Because we did not examine the immunohistochemical analysis of cones due to the lack of antibody to loach cone photoreceptors, we instead performed a spectrophotometric analysis of the photoreceptors in the loach eyes to examine the photoreceptive function of the visual pigments. Characteristic peaks were observed around 410 nm, 540 nm, and 580 nm in the absorption spectrum of the CHAPS-solubilized ocular extract (Fig. 6F, curve 1, “Eyeball extract”), which are indicative of heme proteins, which are widely observed in a variety of animal tissue extracts. We added NH_2OH to the extract for the rapid conversion of photointermediate metaporphyropsin or metarhodopsin, which are formed by light irradiation, into retinal oximes and opsin apoproteins. After judging the termination of the NH_2OH-induced dark reaction from no spectral change (Fig. 6F, curve 2, “100 mM NH_2OH 120 min”), the extract was irradiated with red and green light

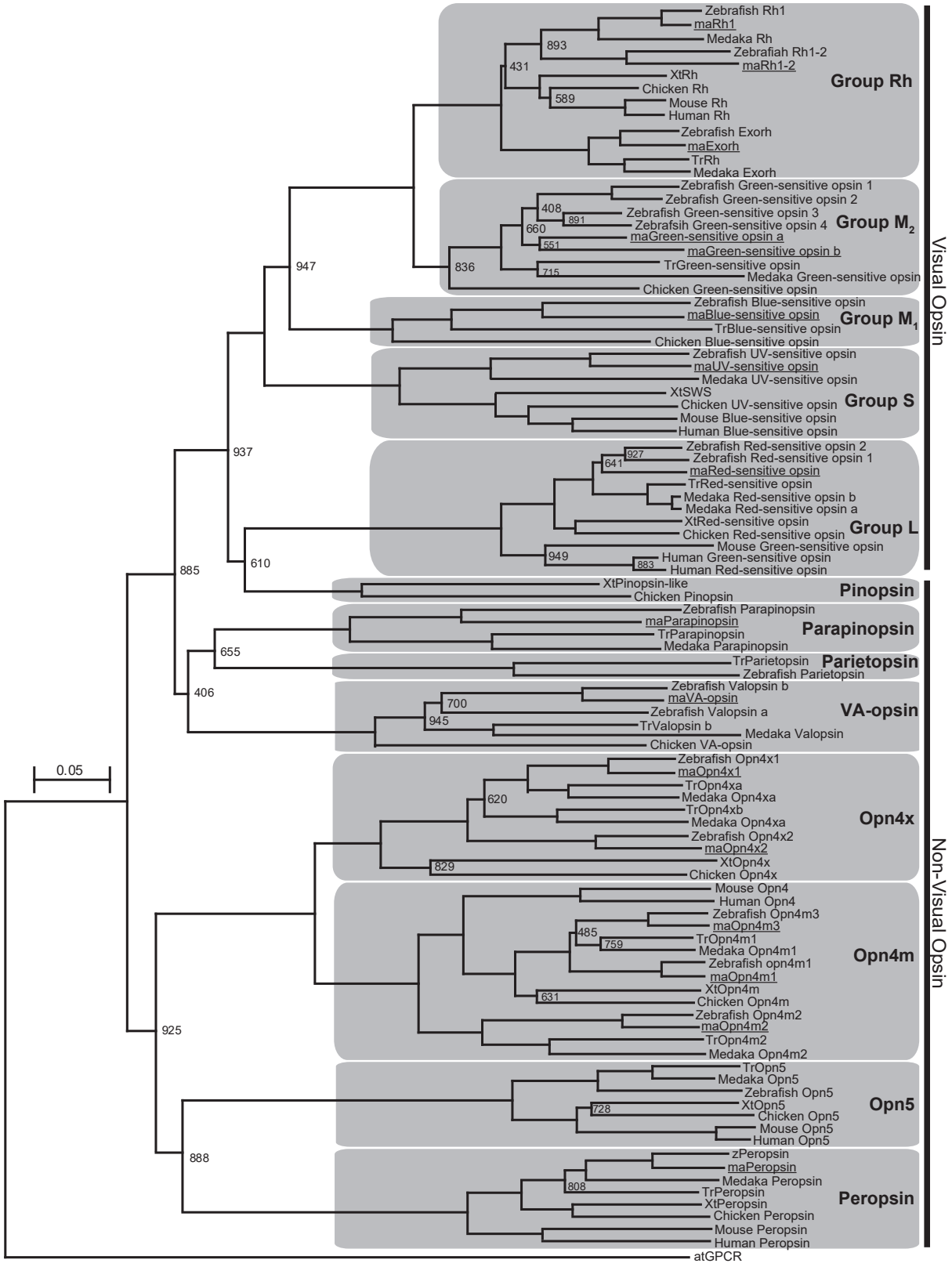

Fig. 5. Molecular phylogenetic tree of loach opsins. The molecular phylogenetic tree was constructed using the Neighbor-Joining method (ClustalW ver. 2.1). The values at the branches indicate bootstrap probabilities. Bootstrap values > 95% are omitted. Multiple alignments were made using MEGA 6.06. Because some of amino acid sequences obtained from the transcriptome database did not cover the entire CDS, the N-terminus and/or C-terminus of the alignment were manually omitted, and then the processed alignment (corresponding to Glu^{3}–Pro^{356} in zRed opsin1) was subjected to progressive alignment by using ClustalW ver. 2.1, (DDBJ) to generate the molecular phylogenetic tree. Tr, *Tetraodon nigroviridis*; Xt, *Xenopus tropicalis*; ma, *Misgurnus anguillicaudatus*; At, *Arabidopsis thaliana*.

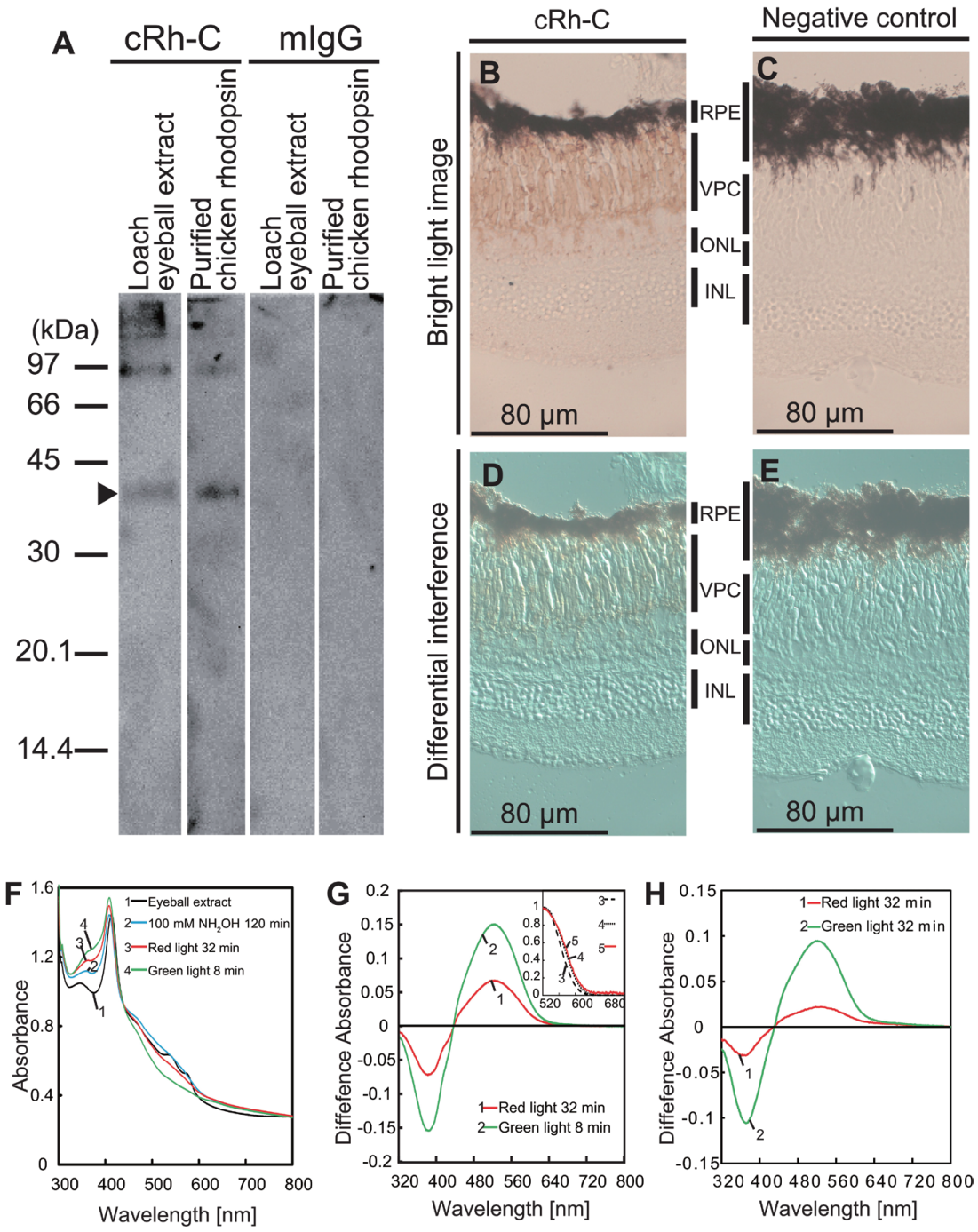

Fig. 6. Immunohistochemical localization and spectrophotometry of Japanese loach rod pigment in the retina. **(A)** Immunoblot analysis of Japanese loach ocular proteins. Arrowhead indicates a presumed monomeric form of loach porphyropsin. Eyeball extracts of Japanese loach containing 704 ng of porphyropsin or purified 4 ng chicken rhodopsin were loaded. **(B)** A bright-field image of Japanese loach retinal section immunostained by anti-chicken rhodopsin cRh-C. **(D)** A differential interference contrast (DIC) image of the same section as in **(B)**. **(C, E)** Control sections using horse normal serum. RPE, retinal pigment epithelium; VPC, visual pigment cells; ONL, outer nuclear layer; INL, inner nuclear layer. **(F)** Absorption spectra of Japanese loach eyeball extract. To the extract ("eyeball extract"), NH_2OH-HCl was added to a final concentration of 100 mM ("100 mM NH_2OH"). Then, the sample was kept in dark for 120 min until the spectral changes dissipated. Subsequently, the sample was successively irradiated with red light (727.0 μW/cm^2, λ_{max} = 660 nm) for 32 min and green light (574.2 μW/cm^2, λ_{max} = 520 nm) for 8 min ("Red light 32 min" and "Green light 8 min"). **(G)** Difference absorbance spectra before the initial irradiation ("100 mM NH_2OH 120 min" in **(F)**) and after each subsequent irradiation ("Red light 32 min" and "Green light 8 min" in panel **(F)**). The inset shows the comparison between the visual pigment templates of λ_{max} = 520 nm and normalized difference absorption spectrum for the spectral changes during red light irradiation for 16 min after a total of 16 min red light irradiation (curve 5). Curve 3 and curve 4 indicate the template spectra of A_1- and A_2-based rhodopsins, respectively. Templates were calculated using the method described in (Okano et al., 1989). **(H)** The sample was prepared separately from Fig. 6F and G. Difference absorbance spectra before the first irradiation and after red light irradiation (202.8 μW/cm^2, λ_{max} = 670 nm: Curve 1) or green light irradiation (158.0 μW/cm^2, λ_{max} = 533 nm: Curve 2).

successively until the spectrum showed no significant changes (total irradiation of 32 min and 8 min, respectively). A green-sensitive pigment, possibly porphyropsin or rhodopsin, was bleached by these irradiations. The difference in spectra was calculated by subtracting each irradiation spectrum (Fig. 6G, curve 3, "Red light 32 min"; curve 4, "Green light 8 min") from that before the irradiation (Fig. 6F, curve 2, "100 mM NH_2OH 120 min"), which provided an absorption maximum at 520 nm. Importantly, they showed an isosbestic point around 440 nm, suggesting the bleaching of a single component.

We did not observe any spectral changes resulting from the red opsins in the spectroscopic analysis, despite the strong signal of the *maRed-opsin* in the RT-PCR analysis of the eye. Thus, we carried out a further spectrophotometric analysis after regenerating the photopigments by the addition of 11-cis-retinal in the dark, since the red-opsin may have been degenerated by the dim-red light used during the sampling (Fig. 6H). However, no spectral changes were detected in the long wavelength region compared with the experiment without the addition of 11-cis-retinal (Fig. 6G and H), implying that the Japanese loach has few red cones in its eyes.

The spectral shapes of retinal photopigments change depending on whether the chromophore is A_1- or A_2-retinal. Therefore, we compared the difference spectra of the green-sensitive component to the templates for A_1- and A_2-retinal-based pigments (Govardovskii et al., 2000). As shown in the inset of Fig. 6G, the difference spectra were precisely matched with the template spectrum calculated for A_2-based rod opsin (porphyropsin), better than that for A_1-based rhodopsin (Fig. 6G, inset). This result coincides with the results of loach retinal analysis by Toyama et al. (Toyama et al., 2008). These findings confirm that the Japanese loach has porphyropsin rather than rhodopsin in their eyes.

In order to estimate the total amount of porphyropsin in a loach eye, we further repeated the extraction of porphyropsin from Japanese loach eyes. The content was estimated to be 0.0073 OD per eyeball. From the sizes of the eyes used for the pigment quantitation, the average surface area of the retina and the density of porphyropsin were calculated to be 0.098 cm^2 and 0.074 OD/cm^2, respectively (Table 3).

Locomotor activity analysis of blinded Japanese loach

In the analyses of the locomotor activity with a 4-hr time window (Supplementary Table S5 and Fig. 7, bottom rows), the locomotor activity was found to decrease in five of eight individuals after removal of the eyes, compared to before the removal (Fig. 7A, B, D, G, and H). However, all individuals seemed to show nocturnal activity, even after enucleation, according to double-plotted actograms (Fig. 7A, B, D, and H; top rows). In fact, chi-squared periodograms showed that all animals had significant 24-hr rhythmicity with periods of 22.5–25.6 hr. These periods are similar to those found in intact animals in LD (Fig. 1, LD and Fig. 7, Intact) rather than intact animals in DD (Fig. 1, DD), A significant difference was not detected between the loaches before and after the enucleation in terms of the amplitudes or period-lengths (Supplementary Figure S9). In addition, the enucleated animals still showed acute light responses just after the lights were turned off (Supplementary Figure S10). These data strongly suggest that Japanese loaches can synchronize their locomotor activity rhythm with the LD cycle without the input of a light signal from the eyes.

DISCUSSION

Regulation of the locomotor activity by light and circadian clock

The present observation of nocturnal locomotor activity of the loach is in part consistent with that reported by a previous study (Naruse and Oishi, 1994), in which Japanese loaches showed nocturnal activity when fed at midnight, with strong activity in the morning (ZT0–ZT6) when fed at noon (ZT6). Furthermore, the feeding affected the activity patterns in the following DD or LD without feeding (Naruse and Oishi, 1994); the dark-active pattern under the scheduled feeding at midnight was maintained in the condition without food, whereas the morning-active pattern under the scheduled feeding at noon did not continue in the subsequent LD condition without food. In the present study, the loaches were fed before measurement and fed only once (day 3, ZT10) during the measurement at late daytime, to minimize the possible effects of feeding time on locomotor activity. Under the present condition, eight of 14 fish showed nocturnal locomotor activity without the anticipatory activity around the end of daytime (Fig. 1A–H) and no individual fish showed clear diurnal activity. Therefore, these results suggest that environmental light is a stronger determinant of the behavioral pattern than feeding time, although we did not determine the precise contribution of feeding schedule to the behavioral pattern.

Under the LD condition, some animals did not show any significant increase of locomotor activity in the dark phase (Fig. 1I–N, top rows), while others showed clear nocturnal behavior (Fig. 1A–H). These non-nocturnal individuals showed lower activity throughout the day (Fig. 1I–L and N; bottom rows), which may be the reason for the technical difficulty in the detection of a significant daily variation. Although it is difficult to measure the behavioral difference between the active and inactive individuals, genetic diversity may play a role in regulating activity levels (Kjaer, 2017). However, no individuals showed any diurnal locomotor activity in the present study, and, therefore, our results suggest that loach locomotor activity is likely to be suppressed by light and weakly regulated by the circadian clock.

Table 3. Features of human, mouse, and loach eyes.

Species	Diameter of eye [cm]	Area of retina estimated as hemisphere [cm^2]	Estimated density of rod visual pigment [ODmL/cm^2]
human			0.35 [1]
mouse	0.33±0.01[2]	0.68[2]	0.46
loach	0.25±0.02	0.098±0.018	0.074

[1] Alpern and Pugh 1974
[2] Lyubarsky et al., 2004

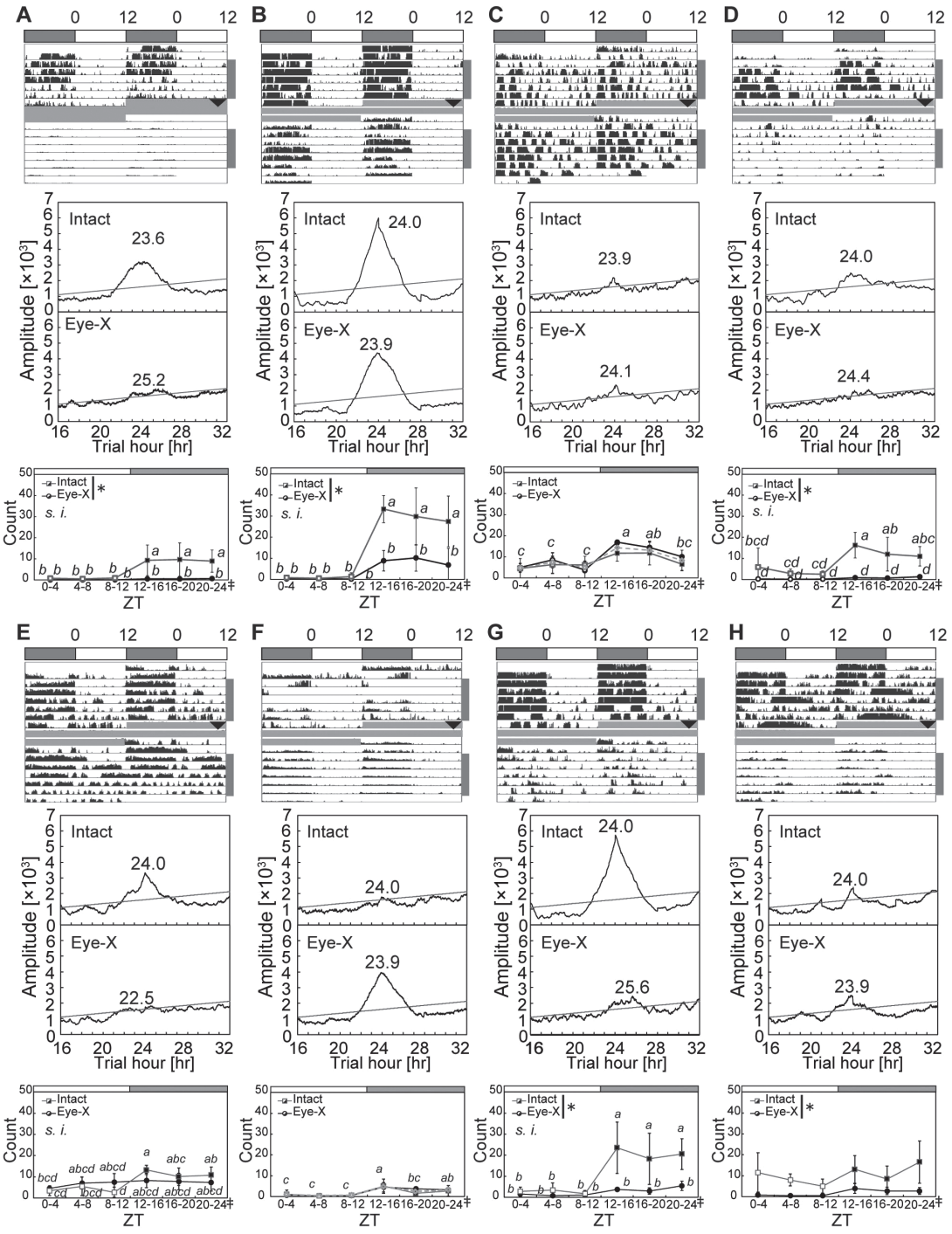

Fig. 7. Locomotor activity of blinded Japanese loach. The locomotor activities of intact fish were measured for seven days in LD (12:12). On day 7, the eyes were enucleated under ice anesthesia at ZT10–ZT11 (black arrow heads) and treated for one day with 50 μg/L malachite green oxalate (grey horizontal lines). Their locomotor activity was subsequently measured for seven days under LD cycles. Top rows: Double-plot actograms of the locomotor activities of eight Japanese loaches. Middle rows: Chi-squared periodograms of the locomotor activities. Significance lines ($P < 0.01$) are colored in grey. The presumed free-running periods are shown. Eye-X; eye excision. Bottom rows: Analyses of the locomotor activities in a 4-hr window. One cycle was divided into six equal periods. Locomotor activities of five daily cycles (shown by grey bars on the right side of double-plot actograms) were averaged for every period (counts ± SD per min). The averaged values of intact fish for dark and light points were plotted by solid and open grey squares, respectively. The averaged values of Eye-X fish for dark and light points were plotted by solid and open black circles, respectively. The significance of the interaction between the circadian rhythm and light conditions was examined using two-way factorial ANOVA and shown as significant interaction (*s.i.*) if $P < 0.05$. Multiple comparison tests were performed using the Tukey-Kramer method. Asterisks and daggers represent significant variations depending on the eye experiment conditions and time periods, respectively. Different letters indicate significant differences between comparisons ($P < 0.05$). Dashed lines represent averaged locomotor activities with intact and Eye-X condition, which were drawn when a significant interaction was not detected. Significant daily variations were detected by two-way factorial ANOVA.

Visual pigment of Japanese loach

The spectral shape of the major photopigment in the loach eye correlated well with that of the template for porphyropsin (Fig. 6G, inset), and the difference absorption maximum of the pigment (520 nm) was very close to that of porphyropsins in the eyes of other freshwater fish species (520–524 nm; Wald, 1939). Based on these results, together with a previous report (Toyama et al., 2008), the main pigment, as observed in the spectroscopy, was porphyropsin.

Mice, a well-known nocturnal animal species, have a rod-dominant retina and poor eyesight (Hensch, 2005; Prusky and Douglas, 2004). Lyubarsky et al (2004) reported that the axial density of rhodopsin and the length of the rod outer segment are 0.019 OD/μm and 24 μm, respectively, whereby, the density of rhodopsin can be calculated to be 0.46 OD/cm^2 (Table 3). Compared with these values, the density of Japanese loach porphyropsin is estimated to be approximately 16% of that of mouse rhodopsin. In addition, Japanese loaches have relatively small eyes (relative to body mass) in contrast to known nocturnal reef fishes, such as the haemulid fish *H. sciurus* and the apogonid fish *P. kauderni*, whose eyes are larger than those of diurnal species due to adaptations to scotopic image formation (Schmitz and Wainwright, 2011). As such, Japanese loaches may have no or reduced vision with specialized eyes for detecting environmental light conditions. In general, nocturnal animals adapt to dark environments using different strategies. Some nocturnal animals have rod-enriched retinas to achieve a high sensitivity of scotopic vision. In other cases, they have small eyes or become blind by developing alternative non-visual sensory systems, such as chemosensory or touch sensory systems. Japanese loaches adopt the latter strategy, because they live in muddy water, where they use well-developed barbels for sensory systems instead of vision to find and capture prey.

Non-visual opsin expressed in loach eyes

In addition to visual opsins, we detected the expression of *Opn4m3* mRNA in the eyes (Fig. 4, lane 17). *Opn4*s (melanopsins) are known as circadian photoreceptors that transmit light signals to the circadian clock system (Lucas et al., 2007; Lucas et al., 2001). *ZOpn4m3* has been reported to be photo-responsive in zebrafish (Davies et al., 2011). Therefore, among the five types of *maOpn4* genes identified in the present study (Fig. 5), *maOpn4m3* is a plausible candidate gene encoding a circadian photoreceptor in loach eyes.

Light-input pathway to regulate the locomotor activity

Despite being small, loach eyes retain both their circadian and photoresponsive functions, and their removal did not have any effect on nocturnal locomotor activity (Fig. 7). However, this is not wholly indicative of the lack of or small contribution of the eyes to behavioral regulation, since extraocular photosensitive tissues, such as the pineal gland or deep brain photosensitive tissues (Moore and Whitmore, 2014; Okano et al., 1994; Vivid and Bentley, 2018; Cassone and Menaker, 1984), may also contribute to the regulation of locomotor activity in parallel with the light-input pathway in the retina. As such, extraocular photoreceptive site(s) should be investigated in future experiments, using local excision or illumination of the brain in living fish.

Under the LD condition, the loaches showed locomotor activity of onsets and offsets which clearly coincided with lights being turned on and off, respectively (Fig. 1). This suggests that environmental light signals are likely transmitted to the central nervous system to control the locomotor activity in a circadian-clock-independent manner, and that the circadian clock weakly affects the locomotor activity, along with the light-dependent pathway(s). Alternatively, the neuronal center regulating the locomotor activity may detect the environmental light directly.

Ecological aspects of light-dependent nocturnal locomotor activity in Japanese loach

The physiological and ecological importance of the strong photic and weak circadian regulation of the locomotor activity in the Japanese loach may be relevant to the desynchronization between the locomotor activity and the internal circadian clock. Such a desynchronization has been reported in a cavefish, *A. mexicanus* (Beale et al., 2013), wherein the circadian clock and light-dependent action may be important factors for the maintenance of internal homeostasis and for the adaptation of the fish to the local light environment in the cave, respectively. Although the Japanese loach does not inhabit a cave environment, its ecological environment may have several aspects in common to cave environments. Japanese loaches prefer to hide in tunnel-shaped tubes in artificial breeding environments, as well as to bury themselves in the sand. This type of behavior, in which they shield themselves from light, may provide them with a strategy for avoiding predation by birds. Indeed, the predators of loaches, such as Japanese crested ibis and Japanese white stork, seem to show diurnal behavior, like many birds (Cassone et al., 2014). Loaches are presumed to hide from predator birds during the daytime and become active, i.e., out of the sand, for eating during the nighttime.

Future perspectives

In this study, we identified clock genes in the Japanese loach and investigated their role in the photic and circadian regulation of the eyes. The analysis of *Opsin* genes and porphyropsin in the eyes suggested their visual and circadian photoreceptive function. However, eye excision experiments demonstrated that the eyes do not play an essential role in the regulation of functional behavior. Rather, taking into consideration the muddy water as the natural habitat of the Japanese loach, it may be interesting to investigate whether its eyes may also be specialized for magnetoreception. In migratory birds, the eyes operate to detect geomagnetic fields, possibly using cryptochromes as magnetoreceptors (Ritz et al., 2000). Geomagnetosensing is also found in the non-migratory animals, such as chicken (Wiltschko et al., 2007; Freire et al., 2005) and zebrafish (Takebe et al., 2012). This study may be of relevance to industrial fisheries. That is, considering that the Japanese loach is a potential food resource that is extraordinarily rich in proteins and vitamins, further ethological and chronobiological experiments would help to establish Japanese loach as an edible model fish.

ACKNOWLEDGMENTS

This work was supported by the Japanese Society for the Promotion of Science (JSPS, No. 17H03710, 18K19348) of Japan awarded to T. O.

COMPETING INTERESTS

The authors have no competing interests to declare.

AUTHOR CONTRIBUTIONS

All authors conceived and designed the experiments. Y. S. and Y. T. performed the experiments. All authors analyzed the data and wrote the manuscript.

SUPPLEMENTARY MATERIALS

Supplementary materials for this article are available online. (URL: https://bioone.org/journals/supplementalcontent/10.2108/zs190110/10.2108.zsj.37.177.s1.pdf)

Supplementary Figure S1. Spectrum of fluorescent light for fish-keeping environment. Intensity: 120–240 μW/cm^2, FL25SS EX-D, Panasonic.

Supplementary Figure S2. Schematic illustration of locomotor activity measurement apparatus. The size of the measuring tank is 210 × 70 × 120 mm. The depth of the water is 90 mm. Infrared sensors (OMRON) were set on the tank wall (15 mm from the bottom (×1), 36 mm from the bottom (×2), and 60 mm from the bottom (×1). Rice paddy sand is on the bottom of the tank for approximately 8 mm. Red circles indicate the infrared sensors. The brown band represents the rice paddy sand.

Supplementary Figure S3. Spectrum of white LED light for locomotor activity measuring tank. Intensity: 134.2–272.0 μW/cm^2, LXK 2-PWC4-0180, Lumileds.

Supplementary Figure S4. Spectrum of LED light for sampling tank. Intensity: 60.4–66.9 μW/cm^2, OSTCXBC1E, OptoSupply.

Supplementary Figure S5. Spectrum of dim red LED light for sampling under the dark condition. Intensity: 11.0–14.6 μW/cm^2, OSR7XNE1E1E, OptoSupply.

Supplementary Figure S6. Spectra of red and green LED lights for spectroscopic analysis. Red: 727.0 μW/cm^2, λ_{max} = 660 nm, OSR7XNE1E1E, OptoSupply. Green: 574.2 μW/cm^2, λ_{max} = 520 nm, OSTCXBCB1E, OptoSupply.

Supplementary Figure S7. Spectra of red and green LED lights for spectroscopic analysis. Red: 202.8 μW/cm^2, λ_{max} = 670 nm, OSR7XNE1E1E, OptoSupply (with optical filter [λ_o = 680 nm, ASAHI SPECTRA]). Green: 158.0 μW/cm^2, λ_{max} = 533 nm, OSTCXBCB1S, OptoSupply.

Supplementary Figure S8. Comparison of rhythmicity of locomotor activity between LD and DD conditions. The locomotor activity rhythmicity and period-length under LD condition in Fig. 1 were compared with those in DD condition using Wilcoxon's signed rank test.

Supplementary Figure S9. Comparison of rhythmicity of locomotor activity between intact and Eye-X conditions. The locomotor activity rhythmicity and period-length of intact condition in Fig. 7 were compared with those of Eye-X condition using Wilcoxon's signed rank test.

Supplementary Figure S10. Light response of blinded Japanese loach. Locomotor activity profiles of blinded Japanese loach in the dusk. Each letter represents an individual in Fig. 7.

Supplementary Table S1. Two-way ANOVA of Japanese loach locomotor activity profile under LD and DD conditions.

Supplementary Table S2. Accession numbers of Japanese loach clock genes.

Supplementary Table S3. Two-way ANOVA of Japanese loach clock gene mRNA levels under LD and DD conditions.

Supplementary Table S4. Accession numbers of Japanese loach *Opsin* genes.

Supplementary Table S5. Two-way ANOVA of blinded Japanese loach locomotor activity profile under the LD condition.

REFERENCES

Alpern M, Pugh EN (1974) The density and photosensitivity of human rhodopsin in the living retina. J Appl Physiol 237: 341–370

Beale A, Guibal C, Tamai TK, Klotz L, Cowen S, Peyric E, et al. (2013) Circadian rhythms in Mexican blind cavefish Astyanax mexicanus in the lab and in the field. Nat Commun 4: 2769

Bolger AM, Lohse M, Usadel B (2014) Trimmomatic: A flexible trimmer for Illumina sequence data. Bioinformatics 30: 2114–2120

Cassone VM, Menaker M (1984) Is the avian circadian system a neuroendocrine loop? J Exp Zool 232: 539–549

Cassone VM, Paulose JK, Harpole CE, Li Y, Whitfield-Rucker M (2014) Avian circadian organization: A chorus of clocks. Front Neuroendocrinol 35: 76–88

Davies WIL, Zheng L, Hughes S, Tamai TK, Turton M, Halford S, et al. (2011) Functional diversity of melanopsins and their global expression in the teleost retina. Cell Mol Life Sci 68: 4115–4132

Freire R, Munro UH, Rogers LJ, Wiltschko R, Wiltschko W (2005) Chickens orient using a magnetic compass. Curr Biol 15: 620–621

Govardovskii VI, Fyhrquist N, Reuter T, Kuzmin DG, Donner K (2000) In search of the visual pigment template. Vis Neurosci 17: 509–528

Grabherr MG, Haas BJ, Yassour M, Levin JZ, Thompson DA, Amit I, et al. (2013) Trinity: reconstructing a full-length transcriptome without a genome from RNA-Seq data. Nat Biotechnol 29: 644–652

Hastings M, O'Neill JS, Maywood ES (2007) Circadian clocks: Regulators of endocrine and metabolic rhythms. J Endocrinol 195: 187–198

Hensch TK (2005) Critical period mechanisms in developing visual cortex. Curr Top Dev Biol 69: 215–237

Huang W, Ramsey KM, Marcheva B, Bass J (2011) Circadian rhythms, sleep, and metabolism. J Clin Invest 121: 2133–2141

Huang S, Cao X, Tian X (2016) Transcriptomic analysis of compromise between air-breathing and nutrient uptake of posterior intestine in loach (*Misgurnus anguillicaudatus*), an air-breathing fish. Mar Biotechnol 18: 521–533

Hurd M, Debruyne J, Straume M (1998) Circadian rhythms of locomotor activity in zebrafish. Physiol Behav 65: 465–472

Inoue J, Sato Y, Sinclair R, Tsukamoto K, Nishida M (2015) Rapid genome reshaping by multiple-gene loss after whole-genome duplication in teleost fish suggested by mathematical modeling. Proc Natl Acad Sci 112: 14918–14923

Kjaer JB (2017) Divergent selection on home pen locomotor activity in a chicken model: Selection program, genetic parameters and direct response on activity and body weight. PLoS One 12: e0182103

Li YL, Weng JC, Hsiao CC, Chou M Te, Tseng CW, Hung JH (2015) PEAT: An intelligent and efficient paired-end sequencing adapter trimming algorithm. BMC Bioinformatics 16: S2

Long Y, Li Q, Zhou B, Song G, Li T, Cui Z (2013) De novo assembly of mud loach (*Misgurnus anguillicaudatus*) skin transcriptome to identify putative genes involved in immunity and epidermal mucus secretion. PLoS One 8: e56998

López-Olmeda JF, Pujante IM, Costa LS, Galal-Khallaf A, Mancera JM, Sánchez-Vázquez FJ (2016) Daily rhythms in the somatotropic axis of Senegalese sole (*Solea senegalensis*): The time of day influences the response to GH administration. Chronobiol Int 33: 257–267

Lucas RJ, Douglas RH, Foster RG (2001) Characterization of an ocular photopigment capable of driving pupillary constriction in mice. Nat Neurosci 4: 621–626

Lucas RJ, Freedman MS, Mun M, Foster RG (2007) Regulation of the mammalian pineal by non-rod, non-cone, ocular photoreceptors. Science 284: 505–508

Luo W, Liu C, Cao X, Huang S, Wang W, Wang Y (2015) Transcriptome profile analysis of ovarian tissues from diploid and tetraploid loaches *Misgurnus anguillicaudatus*. Int J Mol Sci 16: 16017–16033

Lyubarsky AL, Daniele LL, Pugh EN (2004) From candelas to photoisomerizations in the mouse eye by rhodopsin bleaching in situ and the light-rearing dependence of the major components of the mouse ERG. Vision Res 44: 3235–3251

Mahoney MM, Nunez AA, Smale L (2000) Calbindin and Fos within the suprachiasmatic nucleus and the adjacent hypothalamus of *Arvicanthis niloticus* and *Rattus norvegicus*. Neuroscience 99: 565–575

Moore HA, Whitmore D (2014) Circadian rhythmicity and light sensitivity of the zebrafish brain. PLoS One 9: e86176

Naruse M, Oishi T (1994) Effects of light and food as Zeitgebers on locomotor activity rhythms in the loach, *Misgurnus anguillicaudatus*. Zool Sci 11: 113–119

Nunez AA, Bult A, McElhinny TL, Smale L (1999) Daily rhythms of Fos expression in hypothalamic targets of the suprachiasmatic nucleus in diurnal and nocturnal rodents. J Biol Rhythms 14: 300–306

Okano T, Fukada Y, Artamonov ID, Yoshizawa T (1989) Purification of cone visual pigments from chicken retina. Biochemistry 28: 8848–8856

Okano T, Yoshizawa T, Fukada Y (1994) Pinopsin is a chicken pineal photoreceptive molecule. Nature 372: 94–97

Panda S, Hogenesch JB, Kay SA (2002) Circadian rhythms from flies to human. Nature 417: 329–335

Prusky GT, Douglas RM (2004) Characterization of mouse cortical spatial vision. Vision Res 44: 3411–3418

Qin C, Huang K, Xu H (2002) Protective effect of polysaccharide from the loach on the in vitro and in vivo peroxidative damage of hepatocyte. J Nutr Biochem 13: 592–597

Ritz T, Adem S, Schulten K (2000) A model for photoreceptor-based magnetoreception in birds. Biophys J 78: 707–718

Sakata R, Kabutomori R, Okano K, Mitsui H, Takemura A, Miwa T, et al. (2015) Rhodopsin in the dark hot sea: Molecular analysis of rhodopsin in a snailfish, *Careproctus rhodomelas*, living near the deep-sea hydrothermal vent. PLoS One 10: e0135888

Sato Y, Nishida M (2010) Teleost fish with specific genome duplication as unique models of vertebrate evolution. Environ Biol Fishes 88: 169–188

Sato TK, Yamada RG, Ukai H, Baggs JE, Miraglia LJ, Kobayashi TJ, et al. (2006) Feedback repression is required for mammalian circadian clock function. Nat Genet 38: 312–319

Schmid B, Helfrich-Förster C, Yoshii T (2011) A new ImageJ plug-in "ActogramJ" for chronobiological analyses. J Biol Rhythms 26: 464–467

Schmitz L, Wainwright PC (2011) Nocturnality constrains morphological and functional diversity in the eyes of reef fishes. BMC Evol Biol 11: 338

Schwartz MD, Nunez AA, Smale L (2004) Differences in the suprachiasmatic nucleus and lower subparaventricular zone of diurnal and nocturnal rodents. Neuroscience 127: 13–23

Takebe A, Furutani T, Wada T, Koinuma M, Kubo Y, Okano K, Okano T (2012) Zebrafish respond to the geomagnetic field by bimodal and group-dependent orientation. Sci Rep 2: 727

Takeuchi Y, Kabutomori R, Yamauchi C, Miyagi H, Takemura A, Okano K, Okano T (2018) Moonlight controls lunar-phase-dependency and regular oscillation of clock gene expressions in a lunar-synchronized spawner fish, Goldlined spinefoot. Sci Rep 8: 6208

Toda R, Okano K, Takeuchi Y, Yamauchi C, Fukushiro M, Takemura A, Okano T (2014) Hypothalamic expression and moonlight-independent changes of Cry3 and Per4 implicate their roles in lunar clock oscillators of the lunar-responsive Goldlined spinefoot. PLoS One 9: e109119

Toyama M, Hironaka M, Yamahama Y, Horiguchi H, Tsukada O, Uto N, et al. (2008) Presence of rhodopsin and porphyropsin in the eyes of 164 fishes, representing marine, diadromous, coastal and freshwater speciesa qualitative and comparative study. Photochem Photobiol 84: 996–1002

Valente LMP, Moutou KA, Conceição LEC, Engrola S, Fernandes JMO, Johnston IA (2013) What determines growth potential and juvenile quality of farmed fish species? Rev Aquac 5: S168–S193

Vatine G, Vallone D, Gothilf Y, Foulkes NS (2011) It's time to swim! Zebrafish and the circadian clock. FEBS Lett 585: 1485–1494

Vivid D, Bentley GE (2018) Seasonal reproduction in vertebrates: Melatonin synthesis, binding, and functionality using Tinbergen's four questions. Molecules 23: 652–704

Wald G (1939) The porphyropsin visual system. J Gen Physiol 22: 775–794

Wang Y, Hu M, Wang W, Cao L, Yang Y, Lü B, Yao R (2008) Transpositional feeding rhythm of loach *Misgurnus anguillicaudatus* from larvae to juveniles and its ontogenesis under artificial rearing conditions. Aquac Int 16: 539–549

Watari R, Yamaguchi C, Zemba W, Kubo Y, Okano K, Okano T (2012) Light-dependent structural change of chicken retinal cryptochrome4. J Biol Chem 287: 42634–42641

Whitmore D, Foulkes NS, Sassone-Corsi P (2000) Light acts directly on organs and cells in culture to set the vertebrate circadian clock. Nature 404: 87–91

Wiltschko W, Freire R, Munro U, Ritz T, Rogers L, Thalau P, Wiltschko R (2007) The magnetic compass of domestic chickens. J Exp Biol 210: 2300–2310

(Received August 25, 2019 / Accepted December 3, 2019 / Published online April 6, 2020)